

The application of Emissivity Estimation to retrieval of land surface temperature from LANDSAT data

Vyddiyaratnam Pathmanandakumar¹

Abstract

Land Surface Temperature (LST) is an important component in many fields, including global climate change research, urban land use/land cover, geo-biophysical investigations, and as a vital input for climate models. The objective of this research is to develop image processing method of retrieving land surface temperature from LANDSAT data using ArcGISPro. In this study an attempt has been made to estimate LST over Vavuniya district, Sri Lanka, using LANDSAT 5 TM and LANDSAT 8 (OLI & TIRS) satellite data. Two images taken by Landsat-5 TM and Landsat 8- OLI&TIRS satellites were used as the basic data source. These raw images were taken in 1997, and 2021, respectively. First, the raw images were radiometrically and geometrically corrected within the scope of the research. Then, to determine the dimension of the LST variations, LST and Normalized Difference Vegetation Index (NDVI) maps were produced. The variability of retrieved LSTs has been investigated in relation to NDVI values for various land use/land cover (LU/LC) types determined from the Landsat visible and NIR bands. The difference between retrieved LST and the average temperature data from Meteorological station Vavuniya indicates that the technique works by giving an error of about 0.5°C. This proposed method of image processing using ArcGISPro has proved as a dynamic tool to estimate LST using imageries of LANDSAT 5 and LANDSAT 8 and Land surface emissivity. Also, it can be used to understand the impacts of urban development on the environment.

Keywords: Land Surface Temperature (LST), Land Surface Emissivity (LSE), NDVI, Landsat, Remote Sensing (RS)

1 Introduction

The temperature of the surface that can be detected when the land surface is in direct contact with the measuring instrument is known as land surface temperature (LST) (Joshi & Bhatt, 2012). The theoretical basis for remote sensing of LST is based on Planck's law, which states that the total radiative energy released by the ground surface strictly increases with temperature. LST is also known as "skin" temperature or radiometric temperature and should not be confused with near surface air temperature. The LST is a direct measure of how hot or cold the Earth's surface feels to the touch (Hulley et al., 2019; Liang & Wang, 2020). The LST is the temperature of the top few micrometers of the soil surface for bare soil surfaces, and the temperature of the canopy leaves for dense vegetation. It is the temperature of the canopy, the understory (limbs, branches, etc.), and the soil surface when there is scant vegetation. LST is commonly calculated by estimating the surface emitted radiance, which is

¹ Lecturer, Department of Geography, Faculty of Arts & Culture, Eastern University, Sri Lanka. Email: pathmananthakumarv@esn.ac.lk

produced by atmospherically correcting the at-sensor radiance and then inverting the Planck function while accounting for emissivity variation (Hulley et al., 2019).

Because of the simultaneous modification of natural land cover and introduction of urban materials, i.e. anthropogenic surfaces, global urbanization has dramatically reshaped the landscape, with significant climatic repercussions at all scales. The identification and characterization of Urban Heat Island (UHI) is typically based on LST that fluctuates regionally due to land surface cover heterogeneity and other meteorological factors (Joshi & Bhatt, 2012).

Ground surveys would allow for extremely precise Land Use Land Cover (LULC) classification, but they are time-consuming, laborious, and expensive, making remote sensing the obvious and preferred alternative (Jeevalakshmi et al., 2017). Medium spatial resolution data from satellites such as LANDSAT and SPOT are appropriate for mapping land cover or vegetation at the regional local scale. The LANDSAT 8 satellite is equipped with two sensors: the Operational Land Imager (OLI) and the Thermal Infrared Sensor (TIRS) (Hemati et al., 2021; Jeevalakshmi et al., 2017). OLI captures data with a 30m spatial resolution with eight bands located in the visible, near-infrared, and shortwave infrared areas of the electromagnetic spectrum, as well as a 15m panchromatic band. TIR radiance is measured at a spatial resolution of 100m by TIRS, which employs two bands positioned in the atmospheric window between 10 and 12 m (Anandababu et al., 2018; Jeevalakshmi et al., 2017; Singh et al., 2020).

Remote sensing data has been used for understanding spatiotemporal land cover change in connection to fundamental physical parameters such as surface radiance and emissivity data. Since the 1970s, satellite-derived surface temperature data (such as Landsat-5/8) have been used for regional climate assessments at various scales (Orhan & Yakar, 2016; Tran et al., 2006). Since 1972, several researchers have used Landsat satellite data as one of the most prominent sources of LST in the globe (Anandababu et al., 2018; Hemati et al., 2021; Hulley et al., 2019; Jeevalakshmi et al., 2017; Joshi & Bhatt, 2012; Liang & Wang, 2020; Orhan & Yakar, 2016; Singh et al., 2020; Sutariya et al., 2022; Tran et al., 2006). Therefore, images from the Landsat-5 and 8 were employed in this investigation as Landsat -5 TM and Landsat 8-OLI/TIRS acquire Multi-temporal thermal image series. LST generated from remote

sensing data is employed in many fields of science, including hydrology, agriculture, forestry, and oceanography etc. (Orhan & Yakar, 2016; Sutariya et al., 2022).

It is essential to obtain LST and use them in various analyses in order to evaluate the problem linked with the environment (Orhan & Yakar, 2016). The objective of this research is to develop image processing method of retrieving land surface temperature from LANDSAT data using ArcGISPro. In this study an attempt has been made to estimate LST over Vavuniya district, Sri Lanka, from LANDSAT 5 TM and LANDSAT 8 (OLI & TIRS) satellite data using ArcGISPro . The technique presented in this paper is used for estimating the LST of a given LANDSAT 5 and LANDSAT 8 images with the input of the red band, near infrared band (NIR) ,and thermal infrared band 6 and band10 (TIR). TIRS band 11 due to its larger calibration unreliability, only band 10 from Landsat 8 along with band 6 from Landsat 5 was considered in the technique.

2 Description of the Study area

The study area, Vavuniya District, was chosen at random. It is located in northern Sri Lanka with an area of approximately 200,449 Ha (2004.49 Sq km). This equates to 10% of the total land area of the Northern and Eastern Provinces, as well as 3% of the island's total land area. North-Mullaitivu District, South-Anuradhapura District, West-Mullaitivu & Mannar Districts, and East-Trincomalee & Anuradhapura Districts are neighboring districts.

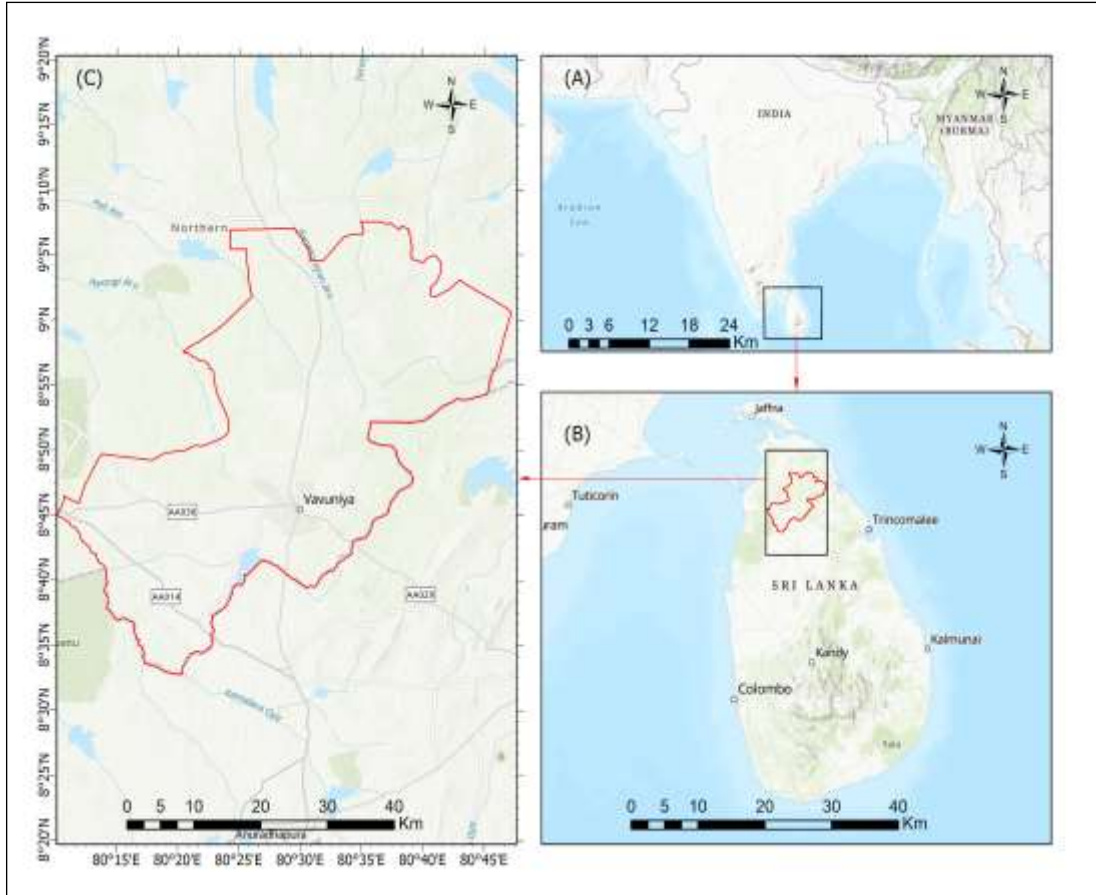


Figure 1: Location map of the study area: (a) Map of South Asia; (b) location of Sri Lanka; and (c) the extend of Vavuniya district

Administratively, Vavuniya district is included in the Wannu Electoral District. This district is divided into four Divisional Secretary divisions and encompasses 102 Grama Niladharies divisions and 505 villages. The district is categorized under the dry zone of Sri Lanka. The climatological conditions are favorable for agriculture. Because of the reddish brown earth, low humid clays, and alluvial soil, the district's soil is extremely fruitful. Bottom lands and concave valleys can be found. The Northern half of the district has red-yellow latro soils, which are more fertile and have better ground water potential. The substrata are determined by hard crystalline rocks with little ground water potential in the other section of the district

3 Data and Methods

Landsat-5 and Landsat-8 multispectral images, as mentioned in Table 1, were used as remote sensing data sources in this study. LST maps were created using cloud-free Landsat-5 and Landsat-8 images obtained in February 2nd 1997 and 2021. Using the UTM projection and the WGS 84 datum, satellite remote sensing data were geometrically transformed to real-world

coordinates during the image processing step. For Landsat-5 and Landsat-8 sensor data, the nearest neighbor resampling method was utilized to generate output images with a ground resolution of 30 m. Band 6 thermal data (120-m) from Landsat-5 and Band 10 thermal data (100 m) from Landsat-8 were re-projected to 30 m using UTM projection and WGS 84 datum. The thermal band was utilized to quantify brightness temperature, while the NIR and RED bands were used to calculate the NDVI.

Table 1: Geospatial data used for change detection analysis of land use and land cover in Vavuniya Divisional Secretariat (in 1997 and 2021)

Datasets	Landsat scene ID	Scale/ Resolution (m)	Year	Data Source
Landsat 5 TM	LT51410541997022BKT01	30 m	1997	US Geological Survey, Earth Explorer
Landsat 8 TM	LC81410542021022LGN00	30 m	2021	US Geological Survey, Earth Explorer

The major steps involved in LST calculation are given in Figure 2.

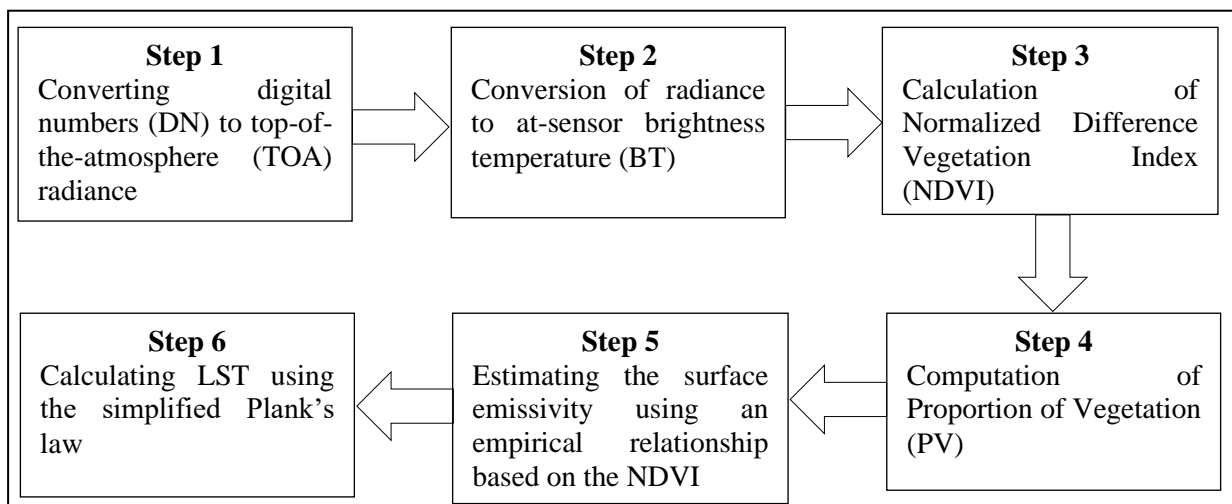


Figure 2: The major steps in LST calculation

3.1 Step 1: Top of atmospheric spectral radiance (TOA)

The initial step in estimating LST was to use band 6 from Landsat-5 and band 10 from Landsat -8 data to estimate top of atmospheric (TOA) spectral radiance (L_λ): To calculate the LST from Landsat-5 thermal infrared band data (band 6), the DN of sensors was converted to spectral radiance using the equation below (Eq. 1) (Orhan & Yakar, 2016).

$$L_\lambda = \frac{L_{max\lambda} - L_{min\lambda}}{Q_{calmax} - Q_{calmin}} \times (Q_{cal} - Q_{calmin}) + L_{min\lambda} \dots \dots \dots (1)$$

Where $L_\lambda =$

Spectral radiance at the sensor's aperture, $Q_{cal} =$ Quantized calibrated pixel value [DN], $Q_{calmin} =$ Minimum quantized calibrated pixel value, $Q_{calmax} =$ Maximum quantized calibrated pixel value, $L_{min\lambda} =$ is the spectral radiance scales to Q_{calmin} , $L_{max\lambda} =$ is the spectral radiance scales to Q_{calmax} . To calculate the LST from Landsat-8 thermal infrared band data (band 10), the DN of sensors was converted to spectral radiance using the following equation (Eq. 2) (Orhan & Yakar, 2016; Sutariya et al., 2022).

$$L_\lambda = M_L * Q_{cal} + A_L \dots \dots \dots (2)$$

Where M_L represents the band-specific multiplicative rescaling factor, Q_{cal} is the Band 10 image, A_L is the band-specific additive rescaling factor.

Table 2: Meta data of Satellite images

Variable	Description	Landsat-5	Landsat-8
Lmax	Maximum and Minimum values of Radiance (Band 6 -Landsat 5), (Band 10 -Landsat 8)	1.238	22.00180
Lmin		15.60	0.10033
Qcalmax	Maximum and Minimum values of Quantize Calibration	255	65535
Qcalmin		1	1
ML	Rescaling factor, (Band 10-Landsat-8)		0.000342
AL			0.1
K1	Thermal constant	607.76	774.89
K2		1260.56	1321.08

3.2 Step 2: Conversion of Radiance to at Sensor brightness Temperature

To estimate the brightness temperature, radiance is converted to at-sensor temperature using the thermal constants provided in the Landsat-8 metadata file (Table 2). The following equation was used to convert spectral radiance to brightness temperature, assuming the earth's surface is a black body (Eq. 3) (Jeevalakshmi et al., 2017; Orhan & Yakar, 2016; Sutariya et al., 2022).

Table 3: Bands properties of Landsat-5 image

Landsat-5			
Bands	Band Name	Wavelength (micrometers)	Resolution (meters)
Band 1	Blue	0.45-0.52	30
Band 2	Green	0.52-0.60	30
Band 3	Red	0.63-0.69	30
Band 4	Near Infrared (NIR)	0.76-0.90	30
Band 5	Short-wave Infrared (SWIR)1	1.55-1.75	30
Band 6	Thermal Infrared	10.40-12.50	120 (30)
Band 7	Shortwave Infrared (SWIR)2	2.08-2.35	30

$$BT = \frac{K2}{\ln\left(\frac{K1}{L\lambda} + 1\right)} - 273.15 \dots \dots \dots (3)$$

Where Tb is the brightness temperature, $L\lambda$ is the cell value as radiance, K1 and K2 are the constants of Landsat-5 and Landsat-8 calibration. The brightness temperature is revised to obtain the results in Celsius by adding the absolute zero (-273.15°C) (Jeevalakshmi et al., 2017; Orhan & Yakar, 2016; Sutariya et al., 2022).

3.3 Step 3: Calculation of Normalized Difference Vegetation Index (NDVI) for Emissivity Correction

The Normalized Difference Vegetation Index (NDVI) is important for identifying the research area's various land cover types. NDVI values vary from -1.0 to +1.0. NDVI is calculated on a per-pixel basis using the formula (Eq. 4) as the normalized difference between the red and near infrared bands of the images. NDVI can be used to determine the amount of vegetation

present and to infer general vegetation status. The NDVI is required for calculating the Proportion of Vegetation (PV), which is closely related to the NDVI, and the emissivity (ϵ) should be determined, which is related to the PV. The following equation can be used to compute NDVI (Eq. 4) (Jeevalakshmi et al., 2017; Orhan & Yakar, 2016; Sutariya et al., 2022).

$$NDVI = \frac{NIR - RED}{NIR + RED} \dots \dots \dots (4)$$

Where, NDVI=Normal Difference Vegetation Index,

NIR = Near-infrared band (Band-5), R = Red band (Band-4)

3.4 Step 4: Computation of Proportion of Vegetation (PV)

This proportional vegetation provides an estimate of the area covered by each land cover category. The NDVI of pure pixels is used to calculate the proportions of vegetation and bare soil. In global conditions, values of $NDVI_v = 0.5$ and $NDVI_s = 0.2$ were proposed. While the value for vegetated surfaces ($NDVI_v = 0.5$) may be too low in some circumstances, $NDVI_v$ can approach 0.8 or 0.9 for higher resolution data over agricultural areas. The following equation can be used to compute Pv (Eq. 5) (Jeevalakshmi et al., 2017; Orhan & Yakar, 2016; Sutariya et al., 2022).

$$Pv = \left(\frac{NDVI - NDVI_{min}}{NDVI_{max} - NDVI_{min}} \right)^2 \dots \dots \dots (5)$$

Where, Pv= Proportion of

Vegetation, NDVI=Normal Difference Vegetation Index, $NDVI_{max}=0.5$, $NDVI_{min}=0.2$.

Table 4: Bands properties of Landsat-8 image

Landsat-8			
Bands	Band Name	Wavelength (micrometers)	Resolution (meters)
Band 1	Coastal aerosol	0.43-0.45	30
Band 2	Blue	0.45-0.51	30
Band 3	Green	0.53-0.59	30
Band 4	Red	0.64-0.67	30
Band 5	Near Infrared (NIR)	0.85-0.88	30
Band 6	SWIR 1	1.57-1.65	30

Band 7	SWIR 2	2.11-2.29	30
Band 8	Panchromatic	0.50-0.68	15
Band 9	Cirrus	1.36-1.38	30
Band 10	Thermal Infrared (TIRS) 1	10.6-11.19	100
Band 11	Thermal Infrared (TIRS) 2	11.50-12.51	100

3.5 Step 5: Estimating the surface emissivity (LSE) using an empirical relationship based on the NDVI

3.5.1 Calculating LSE for Landsat 5

When the NDVI value is less than 0.2, the surface is assumed to be covered with soil, and the emissivity value is set to 0.97. Values between 0.2 and 0.5 are considered soil and vegetation cover mixes. Therefore, Eq. 6 is used to calculate emissivity for soil and vegetation cover mixes. When the NDVI value surpasses 0.5, the surface is considered fully vegetated, and the emissivity value is set to 0.99 (Figure 3) (Orhan & Yakar, 2016).

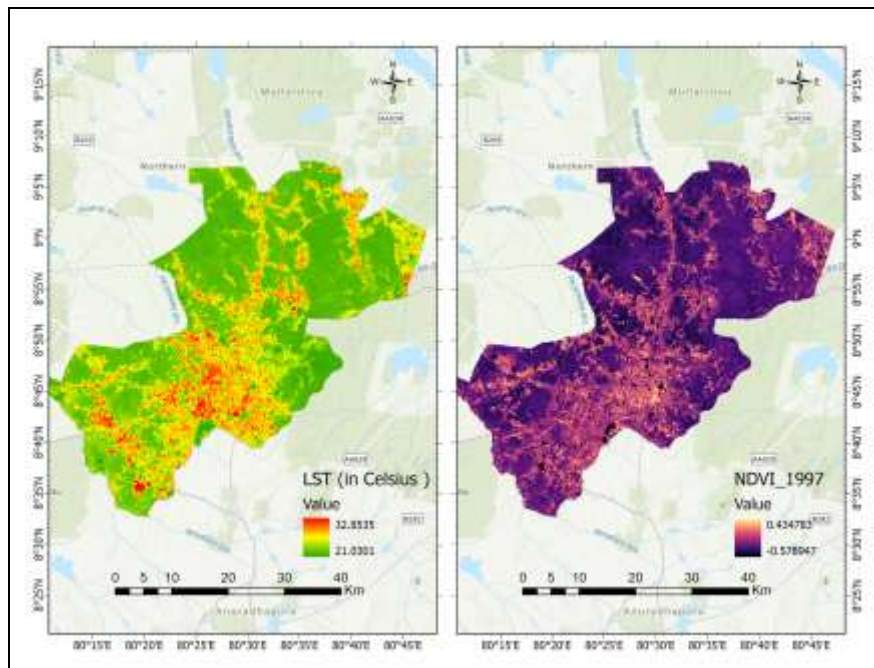


Figure 3: Land Surface Temperature (LST) and NDVI (year 1997)

3.5.2 Calculating LSE for Landsat 8

When calculating LSE, if the NDVI value is less than zero, it is classified as water and an emissivity value of 0.991 is applied. The emissivity value of 0.996 is used for NDVI values between 0 and 0.2, assuming that the land is covered with soil and has no vegetation. For

NDVI values greater than 0.5, it is presumed that the land is vegetated, and the value 0.973 is utilized. Soil and vegetation cover mixtures are assigned a value between 0.2 and 0.5. To compute emissivity, use the formula below (Eq. 6) (Figure 4) (Jeevalakshmi et al., 2017; Orhan & Yakar, 2016; Sutariya et al., 2022).

$$\epsilon = 0.004 * P_v + 0.986 \dots \dots \dots (6) \text{ Where, } \epsilon = \text{Land Surface Emissivity, } P_v = \text{Proportion of Vegetation}$$

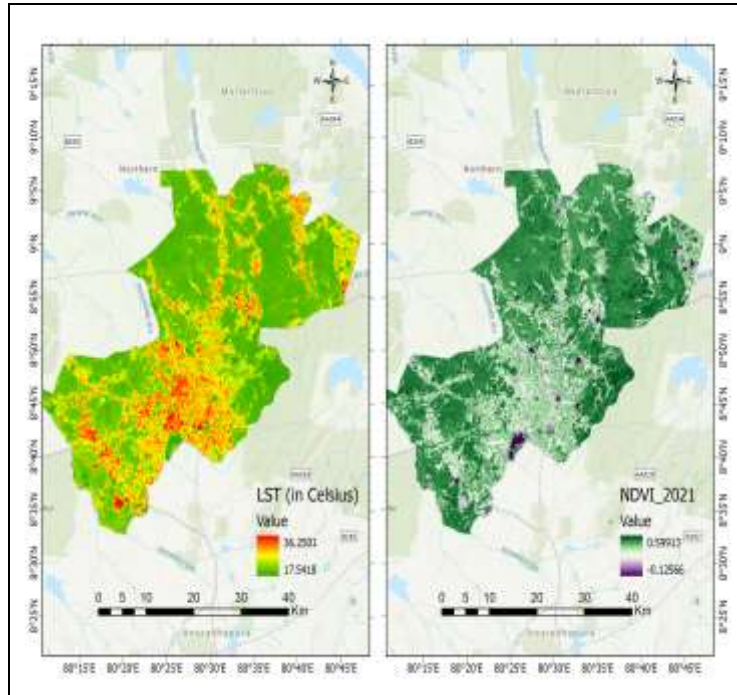


Figure 4: Land Surface Temperature (LST) and NDVI (year 2021)

3.6 Step 6: Land surface temperature Computation

Land surface temperature (LST) is computed using the following equation (Eq. 7) (Jeevalakshmi et al., 2017; Sutariya et al., 2022):

$$T_s = \frac{BT}{(1 + (\frac{\lambda BT}{p}) \ln \epsilon \lambda)} \dots \dots \dots (7)$$

Where λ (11.45 μm for Landsat 4,5 and 7 / 10.895 μm for Landsat 8 band 10 / 12 μm for Landsat 8 band 11) is the emitted radiance wavelength. ρ (0.01438 mK) is generated from the equation $\rho = h * c / b$, in which h ($6.626 * 10^{-34} \text{Js}$) is the Planck's constant, c ($2.998 * 10^8 \text{m/s}$) is the velocity of light, and b ($1.38 * 10^{-23} \text{J/K}$) is the Boltzmann constant, and $\epsilon \lambda$ is the surface emissivity. To accomplish the above estimation, an algorithm was developed in ArcGIS pro for estimation of LST for any other Landsat - 5 and Landsat - 8 image for any other date, the

same algorithm can be executed. The different steps involved in development of the algorithm are presented in Figure 2.

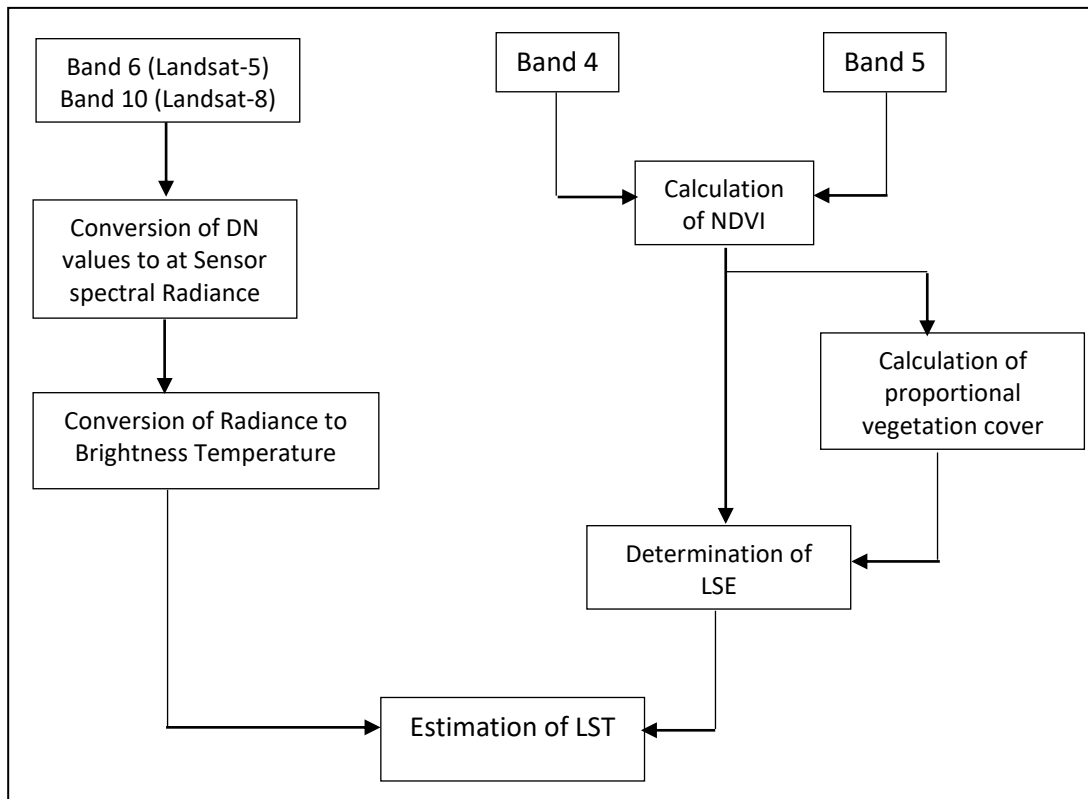


Figure 5: Flow diagram for LST retrieval

4 Result and discussion

The study area Vavuniya district, Sri Lanka, is shown in Figure 1. Satellite images of two dates of the same district were downloaded from the USGS website. The study area chosen includes water, bare soil, vegetation cover and built-up area. Landsat 5 and Landsat 8 data for the dates 02.02.1997 and 02.02.2021 were used for the present study the atmosphere of the study area is comparatively dry and therefore, the range of water vapour values is relatively small. Hence the atmospheric effect is not taken into account in estimating the LST. The temperature hourly data were collected from the Department of Meteorology Vavuniya and are used for comparison with the retrieved LST. The near-surface air temperature of Meteorological station Vavuniya is used for validating the retrieved LST of satellite images. The comparison was made with the air temperature data of Meteorological station Vavuniya. The LST was calculated and taken for the pixel in which the Meteorological station Vavuniya is located. The differences may also be due to some weather conditions and sensor

characteristics of the Meteorological station Vavuniya and another thing that has to be taken into consideration is the location of the thermal sensor. LSTs were retrieved for the downloaded satellite images of 1997 and 2021 using ArcGISPro. For the Vavuniya District, the location of meteorological station of Vavuniya was chosen in keeping view about the cloud pixels and other unwanted events for assessment of accuracy. The retrieved LST was compared with the existing temperature data. The difference between retrieved LST and the existing temperature data for the two dates are shown in Table 5

Table 5: Retrieved LST and meteorological station Vavuniya data for 02.02.1997 and 02.02.2021

Location	Average temperature (°C)		LST retrieved (°C)		Error (°C)	
	1997	2021	1997	2021	1997	2021
Vavuniya meteorological station	28.27	29.01	28.75	29.42	0.48	0.41

5 Conclusion

The model created in ArcGISPro, estimated the LST for the selected datasets over the study area. The algorithm was created using the brightness temperature of band 6 of LANDSAT 5 and band 10 of LANDSAT 8, and the emissivity of different land covers types, derived from visible and near-infrared bands of LANDSAT 5 and LANDSAT 8. The retrieved LSTs were verified using the near-surface temperature data from meteorological station Vavuniya. From the comparison, it has been observed based on the data from meteorological station of Vavuniya that the error calculated for the case of 1997 was 0.48°C and that for the second case it was 0.41°C. The presented technique estimated SLT with minor difference with actual temperature data. These differences can be due to the difference between the resolutions of thermal band 6 of LANDSAT 5 (which is of 120m and visible & NIR band, which is of 30m) and thermal band 10 of LANDSAT 8 (which is of 100m and visible & NIR band, which is of 30m). This paper proposes an ArcGISPro image processing method to estimate LST and can be used to understand the urban development impacts on the environment. This tool has proved as a dynamic tool to estimate LST using the brightness temperature information of LANDSAT 5 and LANDSAT 8 and Land surface emissivity (LSE) from proportional

vegetation cover. In future, the technique to estimate LST can be altered by considering atmospheric effects and weather conditions of seasonal variations by processing the time series data over the area of interest. And also a correlation between NDVI and LST can be demonstrated which helps specifically in urban heat analysis.

6 Reference

- Anandababu, D., Purushothaman, B. M., & Suresh Babu, S. (2018). Estimation of Land Surface Temperature using LANDSAT 8 Data. *International Journal of Advance Research*, 4(2), 177–186. www.IJARIT.com
- Hemati, M., Hasanlou, M., Mahdianpari, M., & Mohammadimanesh, F. (2021). A systematic review of landsat data for change detection applications: 50 years of monitoring the earth. *Remote Sensing*, 13(15). <https://doi.org/10.3390/rs13152869>
- Hulley, G. C., Ghent, D., Göttsche, F. M., Guillevic, P. C., Mildrexler, D. J., & Coll, C. (2019). Land Surface Temperature. In G. Hulley & D. Ghent (Eds.), *Taking the Temperature of the Earth* (1st ed., pp. 57–127). Elsevier. <https://doi.org/10.1016/b978-0-12-814458-9.00003-4>
- Jeevalakshmi, D., Narayana Reddy, S., & Manikiam, B. (2017). Land surface temperature retrieval from LANDSAT data using emissivity estimation. *International Journal of Applied Engineering Research*, 12(20), 9679–9687.
- Joshi, J. P., & Bhatt, B. (2012). Estimating Temporal Land Surface Temperature Using Remote Sensing: a Study of Vadodara Urban Area, Gujarat. *International Journal of Geology, Earth and Environmental Sciences*, 2(1), 123–130. <https://www.cibtech.org/J-GEOLOGY-EARTH-ENVIRONMENT/PUBLICATIONS/2012/Vol 2 No 1/15 - JGEE 008 - BINDU BHATT -.pdf>
- Liang, S., & Wang, J. (Eds.). (2020). Land surface temperature and thermal infrared emissivity. In *Advanced Remote Sensing* (2nd ed., pp. 251–295). Academic Press Elsevier. <https://doi.org/10.1016/b978-0-12-815826-5.00007-6>
- Orhan, O., & Yakar, M. (2016). Investigating land surface temperature changes using Landsat data in Konya, Turkey. *International Archives of the Photogrammetry, Remote Sensing and Spatial Information Sciences - ISPRS Archives*, 41(July), 285–289. <https://doi.org/10.5194/isprsarchives-XLI-B8-285-2016>
- Rapp, D. (2014). *Assessing Climate Change: Temperatures, Solar Radiation and Heat Balance* (3rd ed.). Springer. <https://doi.org/10.1007/978-3-319-00455-6>
- Singh, A., Krishna, A., & Singh, P. (2020). *Study on Generation of Urban Heat Island With Increasing Urban Sprawl in Gautam Buddha Nagar (Noida) Uttar Pradesh , India. July*, 3437–3444.

Sutariya, S., Ankur, H., & Tiwari, M. (2022). Development of Modeler for Automated Mapping of Land Surface Temperature Using GIS and LANDSAT-8 Satellite Imagery. *International Journal of Environment and Geoinformatics*, 9(2), 54–59. <https://doi.org/10.30897/ijegeo.820906>

Tran, H., Uchihama, D., Ochi, S., & Yasuoka, Y. (2006). Assessment with satellite data of the urban heat island effects in Asian mega cities. *International Journal of Applied Earth Observation and Geoinformation*, 8(1), 34–48. <https://doi.org/10.1016/j.jag.2005.05.003>